Pulse front adaptive optics: a new method for control of ultrashort laser pulses

Bangshan Sun,[1] **Patrick S. Salter,**[1] **and Martin J. Booth**[1,2,*]

[1]*Department of Engineering Science, University of Oxford, Parks Road, Oxford,OX1 3PJ, UK*
[2]*Centre for Neural Circuits and Behaviour, University of Oxford, Mansfield Road, Oxford, OX1 3SR, UK*

[*]*martin.booth@eng.ox.ac.uk*

Abstract: Ultrafast lasers enable a wide range of physics research and the manipulation of short pulses is a critical part of the ultrafast tool kit. Current methods of laser pulse shaping are usually considered separately in either the spatial or the temporal domain, but laser pulses are complex entities existing in four dimensions, so full freedom of manipulation requires advanced forms of spatiotemporal control. We demonstrate through a combination of adaptable diffractive and reflective optical elements – a liquid crystal spatial light modulator (SLM) and a deformable mirror (DM) – decoupled spatial control over the pulse front (temporal group delay) and phase front of an ultra-short pulse was enabled. Pulse front modulation was confirmed through autocorrelation measurements. This new adaptive optics technique, for the first time enabling in principle arbitrary shaping of the pulse front, promises to offer a further level of control for ultrafast lasers.

OCIS codes: (320.5540) Pulse shaping; (220.1080) Active or adaptive optics; (320.7120) Ultrafast phenomena.

References and links

1. E. E. Hoover and J. A. Squier, "Advances in multiphoton microscopy technology," Nat. Photonics **7**, 93–101 (2013).
2. P. Kukura, D. W. McCamant, and R. A. Mathies, "Femtosecond stimulated Raman spectroscopy," Annu. Rev. Phys. Chem. **58**, 461–488 (2007).
3. R. R. Gattass and E. Mazur, "Femtosecond laser micromachining in transparent materials," Nat. Photonics **2**, 219–225 (2008).
4. B. Lounis and M. Orrit, "Single-photon sources," Reports Prog. Phys. **68**, 1129–1179 (2005).
5. M. J. Booth, "Adaptive optics in microscopy," Philos. Trans. R. Soc. A **365**, 2829–2843 (2007).
6. J. A. Kubby, *Adaptive Optics for Biological Imaging* (FL: CRC Press, 2013).
7. K. Wang, D. E. Milkie, A. Saxena, P. Engerer, T. Misgeld, M. E. Bronner, J. Mumm, and E. Betzig, "Rapid adaptive optical recovery of optimal resolution over large volumes," Nat. Methods **11**, 1–7 (2014).
8. M. J. Booth, "Adaptive optical microscopy: the ongoing quest for a perfect image," Light. Sci. Appl. **3**, e165 (2014).
9. A. Jesacher and M. J. Booth, "Parallel direct laser writing in three dimensions with spatially dependent aberration correction," Opt. Express **18**, 21090–21099 (2010).
10. Z. Bor, "Distortion of femtosecond laser pulses in lenses and lens systems," J. Mod. Opt. **35**, 1907–1918 (1988).
11. Z. Bor, Z. Gogolak, and G. Szabo, "Femtosecond-resolution pulse-front distortion measurement by time-of-flight interferometry," Opt. Lett. **14**, 862–864 (1989).
12. A. Federico and O. Martinez, "Distortion of femtosecond pulses due to chromatic aberration in lenses," Opt. Commun. **91**, 104–110 (1992).

#238303 Received 20 Apr 2015; revised 7 Jun 2015; accepted 8 Jun 2015; published 17 Jul 2015

13. M. Kempe, U. Stamm, B. Wilhelmi, and W. Rudolph, "Spatial and temporal transformation of femtosecond laser pulses by lenses and lens systems," JOSA B **9**, 1158–1165 (1992).
14. D. Yelin, D. Meshulach, and Y. Silberberg, "Adaptive femtosecond pulse compression," Opt. Lett. **22**, 1793–1795 (1997).
15. W. Amir, T. A. Planchon, C. G. Durfee, and J. A. Squier, "Complete characterization of a spatiotemporal pulse shaper with two-dimensional Fourier transform spectral interferometry," Opt. Lett. **32**, 939–941 (2007).
16. A. M. Weiner, "Femtosecond pulse shaping using spatial light modulators," Rev. Sci. Instrum. **71**, 1929–1960 (2000).
17. A. M. Weiner, "Ultrafast optical pulse shaping: A tutorial review," Opt. Commun. **284**, 3669–3692 (2011).
18. R. Piestun and D. A. Miller, "Spatiotemporal control of ultrashort optical pulses by refractive-diffractive-dispersive structured optical elements," Opt. Lett. **26**, 1373–1375 (2001).
19. U. Fuchs, U. D. Zeitner, and A. Tünnermann, "Hybrid optics for focusing ultrashort laser pulses," Opt. Lett. **31**, 1516–1518 (2006).
20. G. D. Love, "Wave-front correction and production of Zernike modes with a liquid-crystal spatial light modulator," Appl. Opt. **36**, 1517–1520 (1997).
21. P. M. Birch, J. Gourlay, G. D. Love, and A. Purvis, "Real-time optical aberration correction with a ferroelectric liquid-crystal spatial light modulator," Appl. Opt. **37**, 2164–2169 (1998).
22. S. Akturk, X. Gu, E. Zeek, and R. Trebino, "Pulse-front tilt caused by spatial and temporal chirp," Opt. Express **12**, 4399–4410 (2004).
23. P. S. Salter and M. J. Booth, "Dynamic control of directional asymmetry observed in ultrafast laser direct writing," Appl. Phys. Lett. **141109**, 1–4 (2012).
24. F. Druon, G. Chériaux, J. Faure, J. Nees, M. Nantel, A. Maksimchuk, G. Mourou, J. C. Chanteloup, and G. Vdovin, "Wave-front correction of femtosecond terawatt lasers by deformable mirrors," Opt. Lett. **23**, 1043–1045 (1998).
25. E. Zeek, K. Maginnis, S. Backus, U. Russek, M. Murnane, G. Mourou, H. Kapteyn, and G. Vdovin, "Pulse compression by use of deformable mirrors," Opt. Lett. **24**, 493–495 (1999).
26. E. Zeek, R. Bartels, M. M. Murnane, H. C. Kapteyn, S. Backus, and G. Vdovin, "Adaptive pulse compression for transform-limited 15-fs high-energy pulse generation," Opt. Lett. **25**, 587–589 (2000).
27. J. D. Kafka and T. Baer, "Prism-pair dispersive delay lines in optical pulse compression," Opt. Lett. **12**, 401–3 (1987).
28. J. Squier, R. Wolleschensky, U. Simon, and G. J. Brakenhoff, "Dispersion pre-compensation of 15 femtosecond optical pulses for high-numerical-aperture objectives," J. Microsc. **191**, 141–150 (1998).
29. M. Born and E. Wolf, *Principles of Optics* (Cambridge University, 2010), 6th ed.
30. M. J. Booth, T. Wilson, H. Sun, T. Ota, and S. Kawata, "Methods for the characterization of deformable membrane mirrors," Appl. Opt. **44**, 5131–5139 (2005).
31. T. A. Planchon, S. Ferré, G. Hamoniaux, G. Chériaux, and J.-P. Chambaret, "Experimental evidence of 25-fs laser pulse distortion in singlet beam expanders," Opt. Lett. **29**, 2300–2302 (2004).
32. Z. Bor, "Distortion of femtosecond laser pulses in lenses," Opt. Lett. **14**, 119–121 (1989).
33. M. Kempe and W. Rudolph, "Femtosecond pulses in the focal region of lenses," Phys. Rev. A **48**, 4721–4729 (1993).
34. S. Szatmári and G. Kühnle, "Pulse front and pulse duration distortion in refractive optics, and its compensation," Opt. Commun. **69**, 60–65 (1988).
35. S.-W. Bahk, J. Bromage, and J. D. Zuegel, "Offner radial group delay compensator for ultra-broadband laser beam transport," Opt. Lett. **39**, 1081–1084 (2014).
36. R. Netz, T. Feurer, R. Wolleschensky, and R. Sauerbrey, "Measurement of the pulse-front distortion in high-numerical-aperture optics," Appl. Phys. B **70**, 833–837 (2000).
37. J. Jasapara and W. Rudolph, "Characterization of sub-10-fs pulse focusing with high-numerical-aperture microscope objectives," Opt. Lett. **24**, 777–9 (1999).
38. P. Bowlan, P. Gabolde, and R. Trebino, "Directly measuring the spatio-temporal electric field of focusing ultrashort pulses," Opt. Express **15**, 10219–30 (2007).
39. M. K. Trubetskov, M. von Pechmann, I. B. Angelov, K. L. Vodopyanov, F. Krausz, and V. Pervak, "Measurements of the group delay and the group delay dispersion with resonance scanning interferometer," Opt. Express **21**, 6658–69 (2013).
40. P. G. Kazansky, W. Yang, E. Bricchi, J. Bovatsek, A. Arai, Y. Shimotsuma, K. Miura, and K. Hirao, "Quill writing with ultrashort light pulses in transparent materials," Appl. Phys. Lett. **90**, 151120 (2007).

1. Introduction

Ultrafast lasers have become integral to many areas of experimental science, from nonlinear microscopy [1] to ultrafast spectroscopy [2], laser micro-fabrication [3], and quantum optics [4] to name a few. The optimum operation of such systems requires the effective delivery of short

#238303 Received 20 Apr 2015; revised 7 Jun 2015; accepted 8 Jun 2015; published 17 Jul 2015

pulses to a target or specimen. One important source of error in these applications is aberration of the laser phase front (contour of constant phase) due to changes in the optical path length along different parts of the beam. Adaptive optics has been extensively employed to maintain a perfect phase front by counteracting any aberrations introduced into a system, with an associated improvement in resolution and efficiency of the target process [5–9]. In addition to these phase aberrations, distortions to the laser pulse front (contour of constant intensity) can also be introduced by the optical system [10–13]. This form of distortion arises from variation in group delay (GD) across the beam profile with a consequent spreading of the arrival times of pulses at the target. Control of both phase and pulse fronts is required to ensure optimal pulse reconstruction.

Beam shaping using two dimensional reflective elements, such as parabolic mirrors or deformable mirrors (DMs), can provide spatial deformation of the pulse front, but only with a concomitant distortion of the phase front, which makes the laser pulse inappropriate in most applications. In another way, temporal pulse shaping can be employed, whereby the whole beam is spectrally dispersed and the temporal shaping is conducted for each individual spectral component [14–17]. Whilst an essential tool for creating ultra-short pulses, this mode controls the pulse front solely within the temporal (or equivalently spectral) domain, resulting in a modulation which is spatially uniform across the beam. Until now, there has been no realization of flexible spatial pulse front modulation, which has limited the ability to control ultrashort laser pulses.

Currently, adaptive optics elements have only been applied to control the phase of the laser pulse. We here present a new concept of adaptive optics: harnessing extra spatial degrees of freedom for pulse front shaping, through the combination of a diffractive and a reflective adaptive optics element (AOE). Effectively, the phase front and the pulse front for an ultrashort pulse become decoupled allowing independent spatial control of each across a beam. We demonstrate that through adaptive control of the pulse in an ultrafast laser system, a beam could be generated with an arbitrarily shaped pulse front, whilst the phase front remains flat. Autocorrelation measurements using an annular intensity distribution were adopted to demonstrate the relative temporal delay between different parts of the beam. The potential applications for this new adaptive optics method are discussed.

2. Principle

It has previously been realised that combining diffractive and reflective/refractive optics can be a useful concept for static shaping of pulse fronts from an ultrafast laser. The design of specialist optics has allowed the focussing of ultra-short pulses at high numerical aperture with minimal increase to the pulse duration [18, 19]. This static concept can be extended to dynamic control through the inclusion of two adaptive optics elements, one diffractive and another either refractive or reflective. We show here this hybrid dynamic optical system permits adaptive control of both phase and pulse fronts in an ultrashort pulse.

We outline the concept in Fig. 1. A diffractive element, such as a liquid crystal spatial light modulator (SLM) [20, 21], invokes a phase delay on the beam within an interval of 2π radians for a monochromatic wavelength. Large phase shapes can still be implemented through discontinuous jumps in the phase profile where the phase is wrapped from 2π to zero radians between adjacent pixels (Fig. 1(a)). Operating as a phase grating, the device is capable of changing the direction of propagation (the k vector) for the beam. However, the impact of this modulation on the optical path length variations across the beam is negligible (< 3 fs); for the pulse front, the SLM behaves essentially like a plane mirror. Hence on reflection from the SLM, the phase front of the pulse (which is perpendicular to the k vector) can be reoriented, while the pulse front is nearly unaffected. An angle is introduced between the pulse front of the beam and the phase

#238303 Received 20 Apr 2015; revised 7 Jun 2015; accepted 8 Jun 2015; published 17 Jul 2015

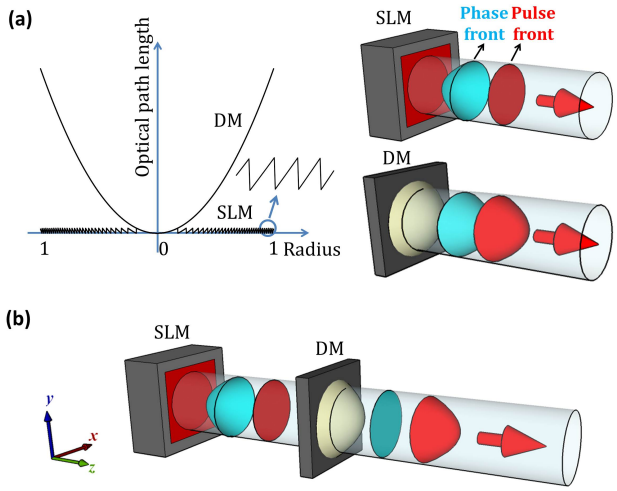

Fig. 1. The principle of adaptive pulse front control. (a) The graph (left) shows the impact of the SLM and DM on the optical path length of the incident light, while the images (right) reveal the associated influence on the phase front and pulse front for an ultrafast beam. (b) The method of combining the SLM with DM to decouple and exert independent control over the phase front and pulse front.

front: a pulse front tilt [22, 23] is created. The spatial multiplexing capability of the SLM may be exploited to generate a local pulse front tilt that varies in both magnitude and orientation for different parts of the beam cross-section, distorting the phase front but without affecting the pulse front shape.

Other adaptive elements, such as a reflective membrane deformable mirror (DM) [24–26], can implement a large phase distortion in a continuous manner, through the introduction of a correspondingly large difference in optical path length (Fig. 1(a)). Thus, both the phase front and pulse front are affected by the DM, such that although distorted, they remain parallel. By combining a reflective DM with a diffractive SLM, it is possible to cancel out any phase front distortion, whilst maintaining the local pulse front tilt. As shown in Fig. 1(b), applying opposite phase shapes to the two adaptive devices, we are able to maintain a flat phase front while generating a spatially variant local pulse front tilt across a collimated beam. Effectively, the pulse front and the phase front have become decoupled within the beam, and through appropriate shaping of the AOEs, it is possible to control each of them independently.

3. The experimental system

The complete system for all the optical measurements is shown in Fig. 2. The laser source used for the experiments was a Titanium Sapphire Oscillator (Newport Spectra Physics Maitai), with central wavelength of 790 nm, 80 fs pulse duration and maximum output power of $\sim$ 300 mW. The power was controlled using neutral density (ND) filters. A pair of prisms [27] was aligned directly after the ND filter to compensate the group velocity dispersion (GVD) effect arising from the optical system [10]. We note higher order dispersion may also exist in the system, however, it was expected to be small since the measured pulse durations before and after the whole optical system were similar. This can in principle be further compensated using prism or grism configurations [28]. The position of the prism pair was finely adjusted to ensure the duration of the pulse exiting the optical system was 80 fs.

#238303 Received 20 Apr 2015; revised 7 Jun 2015; accepted 8 Jun 2015; published 17 Jul 2015

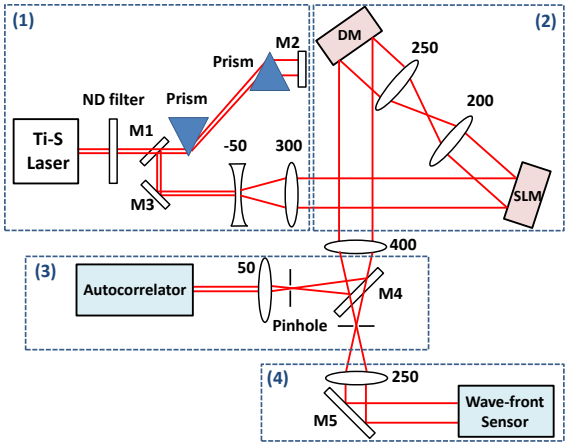

Fig. 2. The optical systems for pulse front shaping and characterization. The pulse front shaping system: (1) the power control and GVD pulse duration compression, (2) the adaptive pulse front control system. The characterization system: (3) autocorrelation measurement, (4) the wave-front measurement. The focal lengths (mm) of the achromatic doublets are shown in the adjacent number. ND filter: neutral density filter, M1 − M5: mirror No. 1 to No. 5, SLM: spatial light modulator, DM: deformable mirror. It should be noted that the diagram is a schematic and does not exactly replicate the experimental optical system.

The laser beam was expanded before illuminating a liquid crystal SLM (Hamamatsu X10468-02). The laser beam expansion was sufficient for the effective region on the SLM to be considered as illuminated with an approximately flat intensity distribution. A 4f lens system was used to image the phase pattern of SLM onto a large stroke DM (Imagine Optic MIRAO 52-e). The SLM is polarization dependent. However, in our configuration it was used purely as a phase modulator.

An autocorrelator (A.P.E Pulsecheck) or a Shack-Hartmann Wave-front Sensor (SHWS; Thorlabs WFS150-7AR) could be coupled in after another 4f system. The autocorrelator was used to demonstrate distortion of the pulse front, while the SHWS was used to verify the correction of phase front aberration. A different 4f lens system was chosen to introduce an appropriate beam size for the autocorrelator or SHWS. A pinhole on an adjustable mount was inserted into the Fourier plane of the DM to block any un-modulated light from the SLM (which forms the zero diffraction order) generated when a large phase pattern was applied. Achromatic doublets were used throughout the system to minimize the system-induced pulse front distortions, enabling us to explore the pulse front solely created by the adaptive optics elements.

4. Phase front characterization

To demonstrate the shaping technique, we generated a quadratic temporal delay of the pulse front with respect to radial position in the beam, since this corresponds to the propagation time delay (PTD) induced on ultra-short pulses by a simple chromatic lens [10]. To implement such a pulse front distortion, it is necessary to apply a quadratic phase of equal magnitude but opposite sign to the SLM and DM. We denote the phase applied for the central wavelength of the laser in the form of the Zernike polynomial [29] $Q(r) = \alpha \cdot \sqrt{3}(2r^2 - 1)$, where α determines the total amplitude of the phase. r is the beam radius normalised to that of the DM, which forms the limiting aperture in this system. The diameter of the DM was 15 mm and, for comparison,

#238303 Received 20 Apr 2015; revised 7 Jun 2015; accepted 8 Jun 2015; published 17 Jul 2015

the $1/e^2$ diameter of the beam at that point was 20 mm. We use the equivalent optical path length ($EOPL$) introduced by dual AOEs to characterize the applied phase magnitude, which is represented by: $EOPL = \lambda \cdot (Q_{\max} - Q_{\min}) / (2\pi)$, where λ is the wavelength of the laser light.

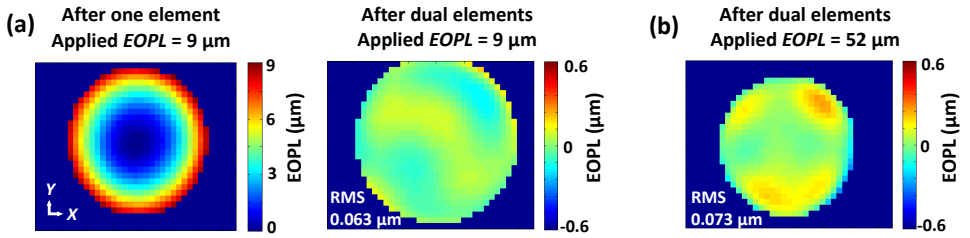

Fig. 3. (a) Example phase fronts measured by Shack-Hartmann Wave-front Sensor, when quadratic phase of $EOPL = 9\ \mu$m was applied to one adaptive optics element (SLM) (left) and dual adaptive optics elements (SLM and DM) (right). (b) The phase front measured for the light when quadratic phase of $EOPL = 52\ \mu$m was applied to SLM and DM.

To generate a pure pulse front distortion while maintaining a flat phase front, it is essential to make sure the phase introduced by the SLM and DM perfectly cancels with each other. Therefore, a Shack-Hartmann wave-front sensor (SHWS) was used to monitor the phase front following the SLM and DM. After calculated phase shapes were initially applied, large amplitude aberrations in the form of Zernike modes were coarsely removed through manual adjustment of AOEs. A feedback loop was then used to update the SLM phase pattern facilitating a modal minimization of the total RMS phase measured by the SHWS. Fig. 3(a) shows the phase front measured by the wave-front sensor when a quadratic phase shape of $EOPL = 9\ \mu$m was applied. It is seen after opposite phases were applied to the dual adaptive elements, an approximately flat phase front (Root-Mean-Square (RMS) of $EOPL = 0.063\ \mu$m) was measured. This is also the case when a large quadratic phase shape was applied to the SLM and DM. An example is shown in Fig. 3(b) with phase of $EOPL = 52\ \mu$m applied to SLM and DM, and phase front with RMS of 0.073 μm was measured for the output beam. It is also seen with increasing the phase amplitude, small amounts of high order residual phase front aberrations may be seen, due to the limited actuator resolution of the DM [30]. In practice, the DM was adjusted in open loop and the SLM updated in closed loop to ensure the total equivalent path length of the phase front measured by the SHWS to be smaller than 0.08 μm RMS, even when applying shapes of $EOPL > 50\ \mu$m. This amount of phase aberration would have an insignificant effect on either the pulse front control or the laser focusing.

5. Pulse front characterization

5.1. Method

The quadratic pulse front generated by dual AOEs was verified by measuring the pulse autocorrelation. To accentuate the effect of the pulse front distortion on the autocorrelation measurement, we implemented a scheme to mask parts of the beam cross-section, measuring only the autocorrelation between two annular regions of differing radius [31]. A phase pattern displayed on the SLM, which is shown in the left image of Fig. 4(a), was applied to generate the annular intensity distribution. A quadratic phase opposite to that introduced by the DM, was displayed only within selected regions of the beam. After reflection from both the SLM and the DM, only the light incident onto these active regions of the SLM has a flat phase front (corresponding to the first diffraction order). Light incident elsewhere on the SLM (corresponding to the zero

#238303 Received 20 Apr 2015; revised 7 Jun 2015; accepted 8 Jun 2015; published 17 Jul 2015

order) propagated with an uncompensated quadratic phase front. A pinhole was aligned in the Fourier plane of the DM (Fig. 2) to spatially filter the strongly defocused zero order. The resultant intensity distribution within the beam measured by a CCD camera is presented in the right image of Fig. 4(a).

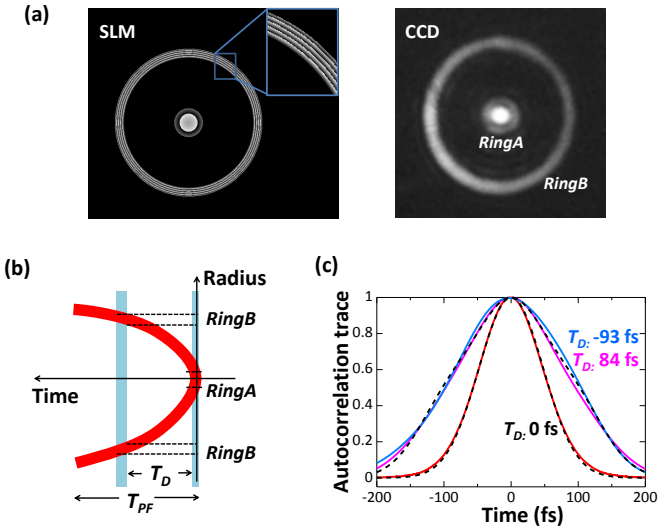

Fig. 4. (a) (left) An example of the phase pattern on SLM to generate double ring-shaped pulses. The inset shows a zoomed in region for the detail. (right) The corresponding annular intensity distribution measured by a CCD camera. (b) A sketch explaining the time delay between pulses from the ring shaped intensity within the beam. (c) The associated autocorrelation measurement for pulses with delays of -93 fs, 0 fs and 84 fs. The measured intensity was normalized for each trace. Dashed curves show the theoretical simulation with T_D set to be $\pm$90 fs and 0 fs.

With a quadratic pulse front, there is a time delay between the two rings of intensity in the beam, as shown in Fig. 4(b). We use T_D to represent the time delay between the two rings, and T_{PF} to represent the time delay between the edge and the center of the beam ($T_{PF} = EOPL/c$, where c is the speed of light). Each ring was narrow enough that it contained minimal pulse front distortion within its width and, hence, the pulse duration within the ring was roughly equal to that of the original laser pulse (80 fs). The two rings were controlled to have similar integrated power, which was achieved by finely adjusting the width of each ring in the experiment. This was also confirmed by measuring the autocorrelation trace intensity for each ring.

When the pulses with intensity in both *RingA* and *RingB* propagated into the autocorrelator, the width of the autocorrelation trace (characterized as full width at half maximum, FWHM) was determined by the amount of the time delay T_D between the two rings. The experimental results of the intensity autocorrelation trace for two rings with different time delays T_D are presented in Fig. 4(c). A quadratic phase of $EOPL = \pm 43$ μm were applied to SLM and DM. A normalized radius of 0.05 was used for *RingA*, while two different radii were adopted for *RingB*: 0.8 and 0.76 predicting T_D to be -93 fs and 84 fs respectively (a positive value represents that *RingB* was delayed with respect to *RingA*). There was an obvious broadening of the autocorrelation trace when the equal and opposite phase shapes were applied to the SLM and DM, demonstrating the presence of pulse front delay. The experimentally measured curves showed close agreement with the simulated autocorrelation trace assuming T_D is equal to 90 fs.

#238303 Received 20 Apr 2015; revised 7 Jun 2015; accepted 8 Jun 2015; published 17 Jul 2015

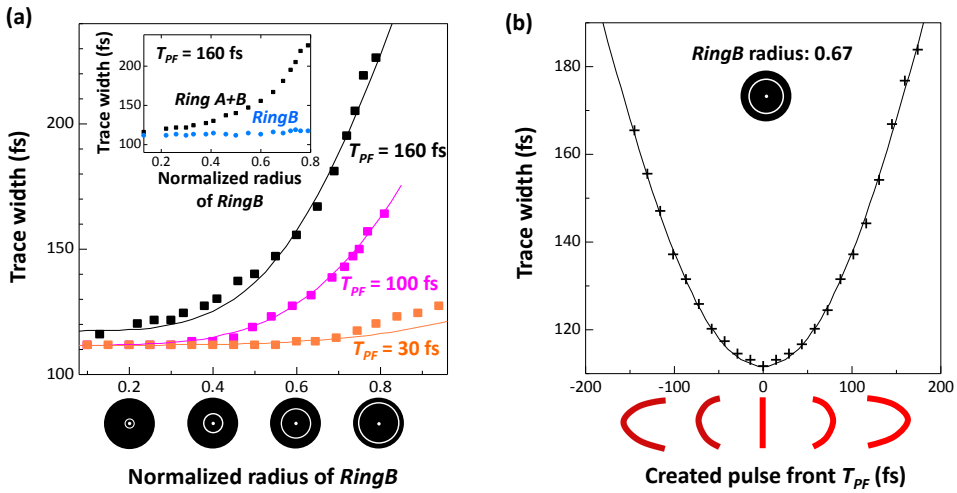

Fig. 5. (a) Graph showing the changes of the autocorrelation trace width with the normalized radius of *RingB*, while *RingA* was fixed at the center of the beam. Dots show measurements; curves are theoretical predictions. Inset: Autocorrelation trace width measured for *RingB* alone, and for *RingA* and *RingB* together. (b) The measured autocorrelation trace width (cross data points) for *RingA* and *RingB* together (*RingB* radius is 0.67), versus the magnitude of created quadratic pulse front. Solid curve is the theoretical prediction. The measurement uncertainty for data points in (a) and (b) was estimated to be $\pm 5\%$.

5.2. *Autocorrelation measurements*

By keeping the position of *RingA* fixed at the center of the beam and varying the normalized radius of *RingB*, we were able to probe the relative temporal delay with respect to position for the rotationally symmetric pulse front distortion. In the experiments of Fig. 5(a), quadratic phase shapes with different amplitudes were applied to dual AOEs. The generated quadratic pulse front was expected to be with magnitude of T_{PF} = 160 fs, 100 fs and 30 fs, respectively. As shown in the three main curves in Fig. 5(a), it is seen that the autocorrelation trace widths obviously increase with the radius of *RingB*. The three solid curves are the simulation assuming the pulse fronts are in perfectly quadratic shapes. The strong match between the experimental and theoretically predicted results proves the creation of quadratic pulse fronts.

Measurements were also performed with just a single ring of intensity, as shown in the inset of Fig. 5(a). The blue dots show the auto-correlation trace width for only *RingB* with an increasing radius, while the trace widths for both rings together ($A + B$, black dots) are added for a comparison. Importantly, the autocorrelation width for a single ring stayed constant at $\sim$114 fs (corresponding to pulse duration of $\sim$80 fs) for all the different radii of *RingB*. This strongly suggests that the pulse duration at each particular radius within the beam was roughly equal to that of the original laser pulse, and the broaden of the autocorrelation trace width is solely introduced by the radially dependent time delay from the quadratic-shape pulse front implemented by dual AOEs.

Due to the adaptive nature of the pulse front shaping, it was straightforward to flexibly adjust the magnitude of the quadratic pulse front. In Fig. 5(b), the created total amount of quadratic pulse front T_{PF} is plotted against measured autocorrelation width. The normalized radius of *RingB* is fixed to be 0.67. The strong match between the experimental and theoretically pre-

#238303 Received 20 Apr 2015; revised 7 Jun 2015; accepted 8 Jun 2015; published 17 Jul 2015

dicted data demonstrates controllability of the pulse front over a large range: the maximum T_{PF} created was 175 fs by applying a phase with $EOPL = 52\ \mu$m to the SLM and the DM.

We therefore conclude that it is possible to shape the pulse front through applying equal but opposite phase fronts to a SLM and DM, and that the pulse front distortion is controllable by varying the magnitude of the phase shape. We note that since the level of pulse front distortion T_{PF} was of the similar order to the original pulse duration, the spatially integrated temporal envelope of the whole beam did not exhibit a significant change. Direct measurement of the entire beam [31] without any annular spatial masking still revealed a broadening of the autocorrelation trace, but the broaden was too small resulting in a much lower resolution for the characterization of pulse front in our situation.

6. Discussion and conclusion

The quadratic shaped pulse front is an important study, since it is the most commonly encountered pulse front distortion in an optical system − the well-known propagation time delay (PTD) [32,33]. However, this technique of pulse front shaping is not simply limited to quadratic profiles. Through proper choice of phase for SLM and DM, in principle pulse fronts with any desired shape and magnitude can be created. Beside the quadratic phase, we additionally applied astigmatism and coma phase with opposite amplitudes to SLM and DM during our investigations. Flat phase fronts were verified by the wavefront sensor, indicating the pulse front with astigmatism and coma shapes were created, although those complex pulse front shapes could not be measured easily by the autocorrelation process.

Although specific lenses or static optical components may be designed to minimize the pulse front distortion in a specific system [18,19,34,35], a significant benefit of this technique allows both the shape and magnitude of the pulse front to be adaptively tuned for any practical scenario. Once fully calibrated, the dynamic response depends on the employed AOEs, and is similar to any adaptive optics optimization routine [6]. Rather than a specific case, this technique could be widely used in any systems with any form of pulse front distortion. Furthermore, the use of adaptive optic elements gives the ability for simultaneous control over the pulse front and phase front in one single system. While creating a desired pulse front, one can introduce an additional phase front through applying a phase pattern to SLM. In this way, the pulse front and phase front can be manipulated at the same time independently of each other.

While these experiments were conducted for the laser with 80 fs pulse duration and 790 nm central wavelength, this pulse front modulation technique is, of course, applicable to lasers of other pulse duration operating in different wavelength bands. A limiting factor moving to lasers of shorter pulse duration will likely relate to dispersion within the SLM. With such effect, the phase front of laser pulses would not be perfectly cancelled by the dual AOEs for all spectral components. However, assuming typical values for the liquid crystal dispersion at a central wavelength of 790 nm, there is expected to only be $\pm$ 2% variation in the $EOPL$ over a 200 nm bandwidth. Therefore, this effect is usually considered to be negligible for most of the lasers. In the future, the advent of new adaptive elements, such as segmented mirror SLMs, are expected to increase the usable bandwidth of the pulse front modulation scheme.

It is well known that the correction of phase front aberrations is beneficial in the applications of ultrafast lasers [5,7,9]. In addition, numerous studies have demonstrated the pulse front distortions generally exist in an optical system, and bring undesired effects, especially when using pulses with shorter durations [10,31,36–39]. However, there have until now been limited studies on the correction of these distortions − primarily due to the absence of an effective method for adaptive pulse front control. The demonstrations in this paper suggest a promising method for the correction of various forms of system-induced pulse front distortions. In addition, the ability to create more complex pulse fronts could possibly bring new and interesting applica-

#238303 Received 20 Apr 2015; revised 7 Jun 2015; accepted 8 Jun 2015; published 17 Jul 2015

tions in laser material processing, where it is already known that pulse front tilt can strongly affect the light-matter interaction [23, 40].

In summary, a new technique using adaptive optical elements to shape the pulse front of an ultrafast laser has been demonstrated. This new ability with in principle arbitrary pulse front shaping could be applied to the correction of a wide forms of pulse front distortions, and open new windows for applications requiring advanced manipulation of ultrashort laser pulses.

Acknowledgments

The authors would like to thank Dr. Alexander Corbett, Dr. Simon Tuohy, Dr. Brian Patton and Dr. Daniel Burke for experimental assistances and valuable discussions. This research was funded by the Leverhulme Trust (RPG-2013-044) and the Engineering and Physical Sciences Research Council (EP/E055818/1).

#238303 Received 20 Apr 2015; revised 7 Jun 2015; accepted 8 Jun 2015; published 17 Jul 2015